LIGAND REGULATION OF THE QUATERNARY ORGANIZATION OF CELL SURFACE M_3 MUSCARINIC ACETYLCHOLINE RECEPTORS ANALYZED BY FLUORESCENCE RESONANCE ENERGY TRANSFER (FRET) IMAGING AND HOMOGENOUS TIME-RESOLVED FRET

Elisa Alvarez-Curto, Richard J. Ward, John D. Pediani and Graeme Milligan

Molecular Pharmacology Group, Neuroscience and Molecular Pharmacology, Faculty of Biomedical and Life Sciences, University of Glasgow, Glasgow G12 8QQ, Scotland, U.K.

Corresponding author: Graeme Milligan, 253 Wolfson Link Building, University of Glasgow, University Avenue, Glasgow G12 8QQ, Scotland, U.K.
Tel: +44 141 330 5557; FAX: +44 141 330 5481 e-mail: g.milligan@bio.gla.ac.uk

Running title: Regulation of muscarinic receptor oligomerization

Flp-In™ T-REx™ 293 cells expressing a wild type human M3 muscarinic acetylcholine receptor construct constitutively and able to express a Receptor Activated Solely by Synthetic Ligand (RASSL) form of this receptor on demand maintained response to the muscarinic agonist carbachol but developed response to clozapine-N-oxide only upon induction of the RASSL. The two constructs co-localized at the plasma membrane and generated strong ratiometric fluorescence resonance energy transfer (FRET) signals consistent with direct physical interactions. Increasing levels of induction of the FRET-donor RASSL did not alter wild type receptor FRET-acceptor levels substantially. However, ratiometric FRET was modulated in a bell-shaped fashion with maximal levels of the donor resulting in decreased FRET. Carbachol, but not the antagonist atropine, significantly reduced the FRET signal. Cell surface homogenous time-resolved FRET, based on SNAP-tag technology and employing wild type and RASSL forms of the human M3 receptor expressed stably in Flp-In™ TREx™ 293 cells, also identified cell surface dimeric/oligomeric complexes. Now, however, signals were enhanced by appropriate selective agonists. At the wild type receptor large increases in FRET signal to carbachol and acetylcholine were concentration-dependent with EC50 values consistent with the relative affinities of the two ligands. These studies confirm the capacity of the human M3 muscarinic acetylcholine receptor to exist as dimeric/oligomeric complexes at the surface of cells and demonstrate that the organization of such complexes can be modified by ligand binding. However, conclusions as to the effect of ligands on such complexes may depend on the approach used.

Monomeric G protein-coupled receptors (GPCRs) have the capacity to bind and activate G proteins (1-3). Despite this, GPCRs also have the capacity to exist as dimers and/or oligomers in living cells (4-7). Such quaternary organization has been suggested, amongst other functions, to play a key role in effective folding and cell surface trafficking of GPCRs (8-10). However, a series of key questions related to GPCR quaternary structure remain to be explored fully. These include the proportion of a GPCR that is dimeric/oligomeric at steady-state, how this may be affected by receptor expression level, if this is regulated at different stages in the lifecycle of a GPCR and the ability of receptor ligands to alter GPCR-GPCR interactions.

Five individual muscarinic GPCRs respond to the neurotransmitter acetylcholine (11, 12). Despite overlapping tissue distribution and very limited selective ligand pharmacology, studies on mouse lines that have selective knock-out of individual muscarinic receptor genes means that a good deal is known about the roles of the individual subtypes (12). For example, the M_3 receptor mediates a wide variety of functions, including vasodilation, bronchoconstriction, stimulation of pancreatic insulin and glucagon release, modulation of salivary gland function and smooth muscle

contraction. An alternative means to study the function of individual muscarinic receptor subtypes is based on the generation of receptor mutants that are often designated Receptors Activated Solely by Synthetic Ligand (RASSLs) (13, 14). The introduced mutation(s) result in loss of affinity for the endogenous ligand but enhanced affinity for one or more small synthetic ligands that have little affinity/potency at the wild type receptor (15, 16). In the case of muscarinic receptors, introduction of mutations at conserved amino acids in transmembrane domains III and V greatly alters the agonist potency ratio between acetylcholine and the synthetic ligand clozapine-N-oxide (17, 18). Expression of such a modified receptor, in either cell lines or in animals via transgenesis, can allow selective activation and analysis of the function and regulation of the RASSL variant.

The quaternary structure of muscarinic receptor family members has been explored extensively (19-24). However, whether ligand binding regulates such interactions is an area of considerable controversy. Using bioluminescence resonance energy transfer (BRET)-based approaches, Goin and Nathanson (21) did not observe short-term agonist regulation of either homo- or hetero-interactions involving M_1, M_2 or M_3 receptors. By contrast, Ilien et al., (25) have reported that the selective M_1 receptor antagonist pirenzepine enhances M_1 receptor dimerization; from a situation where M_1 receptor monomers predominate in the absence of ligand but dimerize upon pirenzepine binding. This is of particular interest because Hern et al., (26) have recently employed modified forms of the antagonist ligand telenzepine in single molecule tracking studies in CHO cells expressing the M_1 receptor. These studies concluded that, any given time, ~30% of the receptor molecules exist as dimers and that this is a dynamic process with the M_1 receptor undergoing inter-conversion between monomers and dimers within seconds. However, if antagonist ligand binding inherently alters such receptor-receptor interactions, then data interpretation may be difficult in studies that rely on imaging of a bound ligand. GPCR quaternary structure has been explored by a number of approaches, but in recent times, these have been dominated by combinations of intact cell BRET and fluorescence-resonance energy transfer (FRET). These techniques are based upon energy transfer between either two auto-fluorescent proteins (in FRET studies) or an auto-fluorescent protein and an enzyme able to generate bioluminescence (in BRET studies). These probes are usually attached to the intracellular C-terminal tail of GPCRs of interest (27-30). Very recently, a novel, homogenous time-resolved (htr)FRET approach has been developed. This takes advantage of the capacity of small proteins based on mammalian O^6-alkylguanine-DNA-alkyltransferase to be covalently modified with fluorescent and other small molecule labels (31). Such 'SNAP' tagging can allow detection of cell surface, as well as intracellular, protein-protein interactions. As a proof of concept, this has been used to explore aspects of GPCR quaternary structure, with particular focus on members of the class C, metabotropic glutamate receptor family (32). Herein, we use combinations of dual color FRET imaging and 'SNAP' tag-based htrFRET of both wild type and RASSL forms of the human M_3 muscarinic receptor to explore the quaternary structure of this receptor and it's potential regulation by ligands.

Experimental Procedures

Materials – Materials for cell culture were from Sigma-Aldrich (Gillingham, Dorset, UK) or Invitrogen (Paisley, Strathclyde, UK). Clozapine-N-oxide was from Biomol International (Exeter, Devon, UK). Other drugs used in this study were from Sigma-Aldrich. Antibodies recognizing the different epitope tags were obtained as listed: anti-c-myc antibody (Cell Signalling, Hitchin, Hertfordshire, UK), anti-SNAP antibody (ThermoFisher Scientific, Epsom, Surrey, UK), monoclonal anti-Flag M2-Peroxidase and anti-Flag M2 monoclonal antibodies were from Sigma-Aldrich. The antiserum directed against VSV-G epitope was produced in-house. All secondary IgG horseradish peroxidise-linked antibodies were from GE Healthcare (Amersham, Buckinghamshire, UK). The radioligand [^{3}H]QNB was from Perkin Elmer (Boston, MA). All oligonucleotides were purchased from ThermoElectron (Ulm, Germany). Flp-In™ T-REx™ 293 cells were from Invitrogen (Paisley, Strathclyde, UK).

Molecular constructs

Generation of the hM$_3$RASSL by site-directed mutagenesis

cDNA corresponding to the human M_3 muscarinic acetylcholine receptor (hM_3) (Accession # AF498917) was obtained from the Missouri S&T cDNA Resource Center (www.cdna.org). This was used as a template to generate the mutated RASSL receptor by substitution of the tyrosine at position 149 with a

cysteine ($Tyr^{149}Cys$), and the alanine in position 239 with a glycine ($Ala^{239}Gly$) as described by Armbruster et al., (17). These mutations were introduced by two sequential rounds of mutagenesis according to the QuickChange II (Stratagene, La Jolla, CA) method using the following primers: $Tyr^{149}Cys$ mutation, 5' GCTTGCCATTGACTGCGTAGCCAGCAATG 3' (forward), 5' CATTGCTGGCTACGCAGTCAATGGCAAGC 3' (reverse); $Ala^{239}Gly$ mutation, 5' GCACAGCCATCGCTGGTTTTTATATGCCT G 3' (forward), 5' CAGGCATATAAAAACCAGCGATGGCTGT GC 3' (reverse). A least 8 clones were screened by DNA sequencing and positives selected and used for further studies.

Flag-hM_3WT-Citrine and myc-hM_3RASSL-Cerulean cDNA constructs

Flag-hM_3WT-Citrine and myc-hM_3RASSL-Cerulean constructs were engineered by the introduction by PCR of Flag or c-myc as N-terminal epitopes. This was followed by subsequent in-frame ligation of the resulting PCR fragments into the EcoRI site of pcDNA3 (Invitrogen) vectors harboring Citrine- or Cerulean-fluorescent proteins respectively. Both Flag-hM_3WT-Citrine and myc-hM_3RASSL-Cerulean fragments were also ligated into pcDNA5/FRT/TO (Invitrogen) to generate stable inducible Flp-In™ T-REx™ 293 cell lines. In both cases the stop codon of the receptor was removed to allow transcription of the fusion protein. The full lengths of the fusion constructs were confirmed to be correct by nucleotide sequencing.

VSV-G-SNAP-hM_3WT and VSV-G-SNAP-hM_3RASSL cDNA constructs

The plasmid pSEMS1-26m (SNAP tag) as supplied by Covalys Biosciences AG/New England Biolabs (Hitchin, UK), was modified by the addition of a small linker region encoding the metabotropic glutamate 5 receptor (mGluR5) signal sequence and an epitope tag (VSV-G) between the Cla1 and EcoR1 sites of the multiple cloning site upstream of the SNAP tag (MCS1). The linker was made by annealing two complementary primers containing the sequences described above with the addition of a Kozak sequence, start codon and appropriate nucleotides to generate Cla1 and EcoRI 'sticky' ends. The primers were annealed by combining 1ng of each with 1x 'multicore' buffer (Promega Corporation) in a final volume of 50µl. This was then heated to 100˚C in a boiling water bath for 5 minutes, after which the bath was then turned off and allowed to cool overnight. The annealed fragment was then purified by gel extraction and ligated into the plasmid by standard techniques. The receptor sequences were PCR amplified using primers designed to add BamHI (5' CGC*GGATCC* *GCCACC* ATG ACCTTGCACAATAACAGT 3') and NotI (5'TTTTCCTTTT*GCGGCCGC*CTA CAAGGCCTGCTCGGGTGC 3') sites to the fragment termini. These were then ligated into the multiple cloning site downstream of SNAP tags (MCS2) of the modified plasmids described above. In order to create constructs which could be used to make Flp-In™ T-REx™ 293 inducible stable cell lines of these constructs, the entire insert from the Cla1 site to the Not1 site was cut out and ligated into a modified version of pcDNA5/FRT/TO (Invitrogen) with a ClaI site added to the multiple cloning site using a linker formed from two annealed primers as described previously.

Generation of stable Flp-In™ T-REx™ 293 cells

Cells were maintained in Dulbecco's modification of Eagle's medium without sodium pyruvate, 4500 mg/liter glucose, and L-glutamine, supplemented with 10% (v/v) fetal calf serum, 1% penicillin/streptomycin mixture, and 10 µg/ml blasticidin in a humidified atmosphere. To generate Flp-In™ T-REx™ 293 cells able to inducibly express the different cDNA constructs, cells were transfected with a 1:9 mixture of cDNA in pcDNA5/FRT/TO vector and the pOG44 vector (Invitrogen) using Effectene (Qiagen, West Sussex, UK), according to the manufacturer's instructions and as described previously (33-35). After 48 h, the medium was changed to medium supplemented with 200 µg/ml hygromycin B (Roche) to initiate selection of stably transfected cells. To constitutively co-express other variants of the hM_3 receptor in the inducible cell lines, these were transfected with the appropriate cDNA construct as described above, and resistant clones selected using 1 mg/ml G418. All stable cell lines were initially screened by fluorescent microscopy for receptor expression and subsequent specific binding of [^{3}H]QNB in cell membranes.

Cell membrane preparation

Pellets of cells were frozen at -80^{o}C for a minimum of 1 hour, thawed and resuspended in ice-cold 10 mM Tris, 0.1 mM EDTA, pH 7.4 (TE buffer) supplemented with Complete

protease inhibitors cocktail (Roche Diagnostics, Mannheim, Germany). Cells were homogenized on ice by 40 strokes of a glass on Teflon homogenizer followed by centrifugation at 1000 x g for 5 min at 4°C to remove unbroken cells and nuclei. The supernatant fraction was removed and passed through a 25-gauge needle 10 times before being transferred to ultracentrifuge tubes and subjected to centrifugation at 50,000 x g for 45 min at 4°C. The resulting pellets were resuspended in ice-cold TE buffer. Protein concentration was assessed and membranes were stored at -80°C until required.

Radioligand binding assays

Saturation binding curves were initiated by the addition of 1μg (hM_3WT) or 5 μg (hM_3 RASSL) of membrane protein to assay buffer (20 mM HEPES, 100 mM NaCl, and 10 mM $MgCl_2$, pH 7.4) containing varying concentrations of [^{3}H]QNB (50.5 Ci/mmol). Non-specific binding was determined in the presence of 10 μM atropine. Reactions were incubated for 90 min at 25^{o}C, and bound ligand was separated from free by vacuum filtration through GF/C filters (Brandel Inc., Gaithersburg, MD, USA). The filters were washed twice with assay buffer, and bound ligand was estimated by liquid scintillation spectrometry.

Cell lysates and Western blotting

Cells were washed once in cold PBS and harvested with ice-cold RIPA buffer (50 mM HEPES, 150 mM NaCl, 1% Triton X-100, and 0.5% sodium deoxycholate, 10 mM NaF, 5 mM EDTA, 10 mM NaH_2PO_4, 5% ethylene glycol, pH 7.4) supplemented with Complete protease inhibitors cocktail (Roche Diagnostics, Mannheim, Germany). Extracts were passed though a 25-gauge needle and incubated for 15 min at 4^{o}C while spinning on a rotating wheel. Cellular extracts were then centrifuged for 30 min at 14000 x g and the supernatant was recovered. Samples were heated at 65^{o}C for 15 min and subjected to SDS-PAGE analysis using 4–12% BisTris gels (NuPAGE, Invitrogen) and MOPS buffer. Proteins were then electrophoretically transferred onto nitrocellulose membranes that were blocked for 45 min in 5 % fat-free milk in TBST (1 x TBS containing 0.1 % (v/v) Tween 20) and subsequently incubated with the required primary antibody overnight at 4^{o}C. Incubation with the appropriated horseradish peroxidase-linked IgG secondary antiserum was performed for 2 hrs at room temperature. Immunoblots were developed by application of enhanced chemiluminescence solution (Pierce Chemical, Rockford, IL USA).

$[Ca^{2+}]_i$ mobilization assays

Cells expressing receptor constructs were grown in clear-bottom black 96 well plates (Greiner Bio-One Ltd, Stonehouse, UK) and for the required length of time. Cells were incubated at 37^{o}C in the dark with the Ca^{2+} sensitive dye Fura-2 diluted to 3 μM in DMEM for 30 minutes. Cells were washed twice with HEPES physiological saline solution (130 mM NaCl, 5 mM KCl, 1 mM $CaCl_2$, 1 mM $MgCl_2$, 20 mM HEPES, and 10 mM D-glucose, pH 7.4) and transferred to a FlexStation II (Molecular Devices, Sunnydale CA) where they were stimulated with different drugs and mobilization of intracellular calcium was recorded as changes of Fura-2 340/380 nm ratio.

Immunocytochemistry

Cells grown on poly-D-lysine-coated coverslips (number 0) were rinsed twice with PBS and cell nuclei were stained by incubating cells for 15 min at 37 °C with fresh PBS containing 10 μg/ml of the nuclear DNA-binding dye Hoechst 33342 (Invitrogen). Samples were then washed 3–4 times with PBS, fixed in a 4% paraformaldehyde/PBS solution for 10 min and washed three times with ice-cold PBS prior to the blocking step performed with 3% (w/v) non-fat dried skimmed milk powder in PBS (non-permeabilized cells) or 3% (w/v) non-fat dried skimmed milk powder plus 0.15% Triton X100 in PBS (permeabilized cells) for 10 min at room temperature. Cells were incubated with the appropriate primary antibody dilution for 1 h (22°C) and subsequently washed twice with PBS. Cells were then incubated for a further 1 h with a dilution of secondary antibody at room temperature. After washing with PBS, coverslips were mounted on to glass slides and viewed using an epifluorescence microscope.

Epifluorescence imaging of SNAP-tag proteins in live cells

Cells stably expressing the receptor of interest were grown on coverslips pre-treated with 0.1 mg/ml poly-D-lysine. SNAP-tag specific substrates were diluted in complete DMEM medium from a stock solution yielding a labelling solution of 5 μM dye substrate. The medium on the cells expressing a SNAP-tag fusion protein was replaced with the labelling solution and incubated at 37°C, 5% CO_2 for 30 minutes. Cells were washed three times with complete medium and a further time with

HEPES physiological saline solution (130 mM NaCl, 5 mM KCl, 1 mM $CaCl_2$, 1 mM $MgCl_2$, 20 mM HEPES, and 10 mM D-glucose, pH 7.4). Coverslips were then transferred to a microscope chamber where they were imaged using an inverted Nikon TE2000-E microscope (Nikon Instruments, Melville, NY) equipped with a 40x (numerical aperture-1.3) oil-immersion Pan Fluor lens and a cooled digital photometrics Cool Snap-HQ charge-coupled device camera (Roper Scientific, Trenton, NJ). For internalization studies, ligands were added to the microscope chamber and fluorescent images were acquired at different time intervals for 40 minutes.

Homogeneous time-resolved FRET studies

Cells expressing the receptors of interest were grown to100000 cells per well in solid black 96 well plates (Greiner Bio-One) pre-treated with 0.1 mg/ml poly-D-lysine. The growth medium was replaced with 100 µl of a mix containing the fixed optimal concentrations of donor and acceptor, Tag-lite SNAP-Lumi4-Tb and Tag-lite SNAP-Red (Cisbio Bioassays, Bagnols-sur-Cèze, France). Plates were incubated for 1 h at 37°C, 5% CO_2 in a humidified atmosphere, and subsequently washed four times in labelling medium (Cisbio Bioassays). Plates were either read directly after this or further processed to test the effect of receptor ligands. For the later experiment, several drug concentrations were added to the plates after being washed in labelling medium; they were then incubated at set temperatures and time and read out on a PheraStar FS (BMG Labtechnologies, Offenburg, Germany) HTRF compatible reader. Both the emission signal from the Tag-lite SNAP-Lumi4-Tb cryptate (620 nm) and the FRET signal resulting from the acceptor Tag-lite SNAP-Red (665 nm) were recorded. Finally, the specific fluorescent signal was calculated by subtracting from the total 665 nm signal that obtained from cells labelled but not expressing the receptor (un-induced cells), and calculating the 665/620 ratio.

Live cell epifluorescence intermolecular Cerulean-Citrine FRET microscopy

Cells were grown on poly-D-lysine treated glass coverslips (number 0) and induced with doxycycline to express the appropriate Cerulean- and Citrine-tagged receptor fusion proteins and tandem positive control constructs. Cells were placed into a microscope chamber containing physiological HEPES-buffered saline solution (130 mM NaCl, 5 mM KCl, 1 mM $CaCl_2$, 1 mM $MgCl_2$, 20 mM HEPES, and 10mM D-glucose, pH 7.4). Cells were then imaged using an inverted Nikon TE2000-E microscope (Nikon Instruments) equipped with a 40 x (numerical aperture = 1.3) oil immersion Fluor lens and a cooled digital photometrics CoolSnap-HQ, (Roper Scientific, Trenton, NJ), attached to the left hand microscope port or a CoolSnap-HQ2 connected to the bottom port. Excitation light was generated from a computer-controlled Optoscan monochromator (Cairn Research, Faversham, Kent, UK) which was coupled to an ultra-highpoint intensity 75 W xenon arc Optosource lamp (Cairn Research). Monochromator was set to 430 and 500 nm for the sequential excitation of Cerulean- and Citrine-tagged receptors or fused and non-fused Cerulean and Citrine respectively. Excitation light was reflected through the Fluor objective lens using a CFP/YFP dual band dichroic (Semrock; Rochester, NY, Cat No-: FF440/520-Di01). Using the multiple dimensional wavelength acquisition module of MetaMorph, acceptor, FRET and donor channel images were acquired using the same exposure time, (175 msec or 250 msec), and were detected using either a high-speed emission filterwheel (Prior Scientific Instruments, Cambridge, UK) coupled to a 12 bit mode Cool Snap-HQ digital camera, (left hand port), or a Quadview 2, (QV2), image splitting device attached to a Cool Snap-HQ2 camera operated in 14-bit mode, (bottom port). Using the emission filter wheel configuration, acceptor, FRET and donor signals were sequentially detected using 542/27 nm and 472/30 nm emitters supplied by Semrock. Detection of equivalent signals using the QV2 image splitter was achieved using the following Chroma, (Chroma**,** Brattleboro, VT), ET series dichroic and emitters: ET t505LPXR dichroic, ET535/30m, ET 470/30m. The image splitting device had the advantage that the FRET and donor signals could be acquired simultaneously without any potential threat of motion. Exposure time, binning, (2 x 2), and camera gain were kept constant for all acquisitions taken during each experiment. Computer control of all electronic hardware and camera acquisition was achieved using Metamorph software (version 7.6.3 Molecular Devices, Sunnydale, CA).

FRET signal correction and normalization of the FRET signal to donor and acceptor FP expression levels

Saved acceptor, FRET and donor channel images were background subtracted and net corrected FRET values from raw FRET images were corrected using Youvan's fully specified

bleedthrough algorithm (36): Net corrected FRET=Raw FRET-[Acceptor-(DA x Donor)] x [AF]-[Donor-(AD x Acceptor)] x [DF], where DA and AD represent the proportion of donor or acceptor bleedthrough, (BT) into the acceptor and donor channel respectively. AF and DF represent the amount of acceptor and donor contamination in the raw FRET signal channel. All BT coefficients were calculated from control cells expressing Cerulean or Citrine alone.

Net corrected FRET values were ratiometrically normalized to the amount of donor and acceptor FP expressed to generate a final ratiometric value, (RFRET) which was dependent on protein expression levels. For this purpose, the equation RFRET=Raw FRET/[Acceptor-(DA x Donor)] x [AF] + [Donor-(AD x Acceptor)] x [DF] was used. Knowing the expected bleedthrough of the donor and acceptor into the FRET channel; therefore in the absence of energy transfer, RFRET will have a predicted value of 1. Values greater than 1 reflect the occurrence of FRET. Quantified RFRET values provided markedly better data quality compared to other ratiometric FRET metric algorithms (37).

RESULTS

The human M_3 muscarinic acetylcholine receptor was modified at the N-terminus to incorporate the Flag-epitope tag and at the C-terminus via in-frame fusion of the modified yellow fluorescent protein Citrine. This generated the Flag-hM_3WT-Citrine construct. Incorporation of Tyr 149 Cys (position 3.33) and Ala 239 Gly (position 5.46) mutations has been reported to generate a form of the M_3 muscarinic receptor with substantially reduced potency for the endogenous agonist acetylcholine but which is able to bind and respond to the synthetic ligand clozapine-N-oxide (25). This form of the M_3 muscarinic receptor was modified at the N-terminus to incorporate the c-myc epitope tag and at the C-terminus via in-frame fusion of the modified cyan fluorescent protein Cerulean. This generated the myc-hM_3RASSL-Cerulean construct. Each of these constructs was inserted into the Flp-In locus of Flp-In^{TM} T-REx^{TM} 293 cells and pools of positive cells selected. No visible expression of either construct was observed in the absence of the antibiotic doxycycline (**Figure 1A, 1B**). However, sustained addition of doxycyline resulted in expression of each form as monitored by fluorescence corresponding to the Citrine- and Cerulean-fluorescent proteins respectively (**Figure 1A, 1B**). Imaging of such cells suggested that the bulk of each construct was located at the plasma membrane (**Figure 1A, 1B**). In functional studies measuring ligand-induced elevation of $[Ca^{2+}]_i$ cells harboring Flag-hM_3WT-Citrine at the Flp-In locus, but in which expression of the receptor construct had not been induced, clozapine-N-oxide was without effect at concentrations up to 1 x 10^{-4}M. This was unaltered by treatment with doxycycline (up to 1 $\mu g.ml^{-1}$, 24h) to induce receptor expression (**Figure 1C**). By contrast, a weak response to carbachol could be recorded in untreated cells, with estimated EC_{50} > 1 x 10^{-4}M. This may reflect either low levels of endogenous expression of the M_3 muscarinic receptor, as has been reported previously in HEK293 cells (38), or low level expression of the construct in the absence of doxycycline. Following induction of Flag-hM_3WT-Citrine a robust response to carbachol was observed with EC_{50} 4.0 +/- 0.8 x 10^{-7}M (mean +/- SEM, n = 4) **(Figure 1C**). As anticipated, both in the absence and presence of doxycycline, Flp-In^{TM} T-Rex^{TM} cells harboring myc-hM_3RASSL-Cerulean displayed no response to carbachol at concentrations up to 1 x 10^{-4}M (**Figure 1D**). A very weak response to clozapine-N-oxide was observed in these cells in the absence of doxycycline (**Figure 1D**). However, a robust response to clozapine-N-oxide with EC_{50} = 1.5 +/- 0.3 x 10^{-8}M (mean +/- SEM, n = 3) developed following induction of myc-hM_3RASSL-Cerulean by treatment with doxycycline (**Figure 1D**). Saturation [^{3}H]QNB binding studies demonstrated that Flag-hM_3WT-Citrine bound this ligand with K_d = 68 +/- 33 pM (mean +/- SEM, n = 4), similar to values reported for the unmodified receptor. myc-hM_3RASSL-Cerulean had almost 40 fold lower affinity (K_d = 2.64 +/- 0.24 nM, mean +/- SEM, n = 4) for this ligand. To assess if this reduction in affinity for [^{3}H]QNB was also noted for other muscarinic antagonists, the affinity of atropine as a competitive antagonist at both Flag-hM_3WT-Citrine and myc-hM_3RASSL-Cerulean was assessed by Schild analysis. Herein, the ability of a range of concentrations of atropine to shift concentration-response curves to carbachol or clozapine-N-oxide respectively was measured. Analysis of such studies produced estimates of affinity for atropine of 3.3 x 10^{-9}M for the wild type receptor and 9.5 x 10^{-9}M for the RASSL, confirming the somewhat lower affinity of atropine for the RAASL mutant that had been described previously (17).

Cells harboring myc-hM3RASSL-Cerulean at the Flp-In locus were subsequently further transfected with Flag-hM_3WT-Citrine. Clones

expressing this construct constitutively and stably were then isolated. Flag-hM_3WT-Citrine was predominantly present at the plasma membrane (**Figure 2A**), whereas, treatment with doxycycline was required for turn-on of expression of myc-hM_3RASSL-Cerulean in these cells (**Figure 2A**). Induction of expression of myc-hM_3RASSL-Cerulean was time-dependent, reaching maximal levels within 24h (**Figure 2B**). This, however, had little effect on the expression level of Flag-hM_3WT-Citrine (**Figure 2B**). As anticipated, based on the pharmacological characteristics of cells able to express each variant individually, in these cells carbachol was an effective and potent agonist in both the absence (EC_{50} = 2.4 +/- 1.3 x 10^{-8}M, mean +/- SEM, n = 3) and presence (EC_{50} = 3.7 +/- 0.14 x 10^{-8}M, mean +/- SEM, n = 3) of doxycycline (**Figure 2C**). By contrast, clozapine-N-oxide was more than 650 fold more potent (EC_{50} = 5.5 +/- 0.8 x 10^{-8}M, mean +/- SEM, n = 3) following treatment with doxycycline (**Figure 2C**). Merging of images of the location of Flag-hM_3WT-Citrine and myc-hM_3RASSL-Cerulean in cells induced to express the RASSL construct indicated almost perfect overlap of localization of the two forms at the cell surface (**Figure 2D**).

Such 'co-localization' studies can only define proximity within a distance of some 300 nm due to the current limits of light microscopy. To explore potential direct interactions between these two forms of the hM_3 receptor FRET imaging studies (**Figure 3**) were performed and both corrected and ratiometric FRET values calculated (**Figure 3A, B**). Both of these calculations indicated that the visual overlap of distribution of the two hM_3 receptor variants was consistent with the formation of Flag-hM_3WT-Citrine-myc-hM_3RASSL-Cerulean dimers/oligomers. The ability of differing concentrations of doxycycline to induce varying amounts of the FRET energy donor myc-hM_3RASSL-Cerulean was assessed by each of cell imaging (**Figure 3A**), direct measures of fluorescence intensity corresponding to the Cerulean fluorescent protein (**Figure 3C**) and anti-c-myc immunoblotting studies (**Figure 3D**). Maintained levels of Flag-hM3WT-Citrine in these cells were similarly confirmed by each of cell imaging (**Figure 3A**), assessing fluorescence intensity corresponding to the Citrine fluorescent protein (**Figure 3C**) and anti-Flag immunoblotting (**Figure 3D**). Both corrected FRET and ratiometric FRET were then calculated at varying acceptor to donor ratios in these cells. These initially increased, from a lack of measurable signal in the absence of donor to reach a peak after exposure to 100 ng.ml^{-1} doxycycline, after which FRET signals were reduced with turn-on of higher levels of myc-hM_3RASSL-Cerulean (**Figure 3B**). Interestingly, addition of carbachol (1 x 10^{-3}M), but neither clozapine-N-oxide (1 x 10^{-4}M) nor atropine (1 x 10^{-5}M), reduced substantially the calculated ratiometric FRET signals (**Figure 3E).** This is consistent with carbachol altering the organizational structure of the oligomeric complex.

FRET between pairs of fluorescent proteins linked to polypeptides of interest is a well characterized means to observe protein-protein interactions in living cells (28-29). However, a novel form of homogenous time-resolved FRET (htrFRET), based on SNAP-tagging, and marketed as TagLite™ (32), has recently been introduced. This is suitable to monitor cell surface protein-protein interactions without the need for antibodies that, because of their potential to induce clustering, have been suggested to limit interpretation of more traditional time-resolved FRET techniques (28). We generated a generic plasmid to allow expression of constructs containing an N-terminal leader sequence, derived from the metabotropic glutamate 5 receptor, linked in-frame to the VSV-G epitope tag sequence, the 20 kDa SNAP tag (31) and then the receptor of interest. Both the wild type and the RASSL forms of the hM_3 receptor were cloned into this plasmid and these were used to generate lines able to express, in an inducible fashion, VSV-G-SNAP-hM_3WT or VSV-G-SNAP-hM_3RASSL (**Figure 4A**). Addition of an anti-SNAP-Alexa-594 labelled antibody to non-permeabilized cells identified, in both cases, cell surface receptors following induction (**Figure 4A**). Furthermore, addition of the cell-permeant SNAP-505 substrate, which links covalently to the SNAP tag, allowed detection of a small pool of intracellular receptors as well as confirming the extensive population of cell surface receptors (**Figure 4A**). Merging of images derived from cells labelled with either the anti-SNAP antibody or SNAP-505 confirmed both cell surface and intracellular pools of the hM_3 receptor variants (**Figure 4A**). Importantly, the presence of the N-terminal leader and SNAP tag did not alter basic pharmacological characteristics of the receptors. Saturation [^{3}H]QNB binding studies indicated a K_d of 54 +/- 5 pM (mean +/- SEM, n = 6) for VSV-G-SNAP-hM_3WT and 2.44 +/- 0.16 nM (mean +/ - SEM, n = 4) for VSV-G-SNAP-hM_3RASSL. Addition of carbachol (1 x 10^{-3}M)

resulted in internalization of 17.9 +/- 1.2 % of cell surface VSV-G-SNAP-hM_3WT over a 40 min period whilst clozapine-N-oxide (1 x 10^{-4}M) produced loss of 17.6 +/- 3.54 % of VSV-G-SNAP-hM_3RASSL over the same time period (**Figure 4B**). By contrast, treatment of either cell line with the agonist selective for the other receptor variant did not produce significant internalization (**Figure 4B**).

To establish optimal conditions for the Tag-Lite™ htrFRET studies, cells induced to express either VSV-G-SNAP-hM_3WT or VSV-G-SNAP-hM_3RASSL were incubated with the terbium-cryptate energy donor SNAP-Lumi4-Tb. The extent of labelling with this reagent was dependent on the level of receptor expression because treatment of cells with concentrations of doxycyline between 0-10 ng.ml^{-1} increased the binding of a range of concentrations of this label (5-30 x 10^{-9}M) in an essentially linear fashion (**Figure 5A and not shown**). Optimization of htrFRET signals corresponding to cell surface hM_3 dimers/oligomers was achieved by varying the added concentration of the corresponding energy acceptor, SNAP-Red, in the presence of a fixed concentration of SNAP Lumi4-Tb (**Figure 5A, 5B)**. For both the VSV-G-SNAP-hM_3WT and VSV-G-SNAP-hM_3RASSL cell lines (**Figure 5B)** this was approximately 8 x 10^{-8}M (**Figure 5A, 5B)** and essentially unaffected by the level of receptor expression (**Figure 5A)**. htrFRET signals were then monitored in cells induced to express VSV-G-SNAP-hM_3WT after addition of a combination of SNAP Lumi4-Tb and SNAP-Red. Basal signal, consistent with the presence of constitutive cell surface hM_3 receptor dimers/oligomers, remained stable over a period of at least 40 min (**Figure 6A**) and was unaffected by the presence of atropine (**Figure 6A**). Interestingly, however, the htrFRET signal was increased substantially by the addition of carbachol (1 x 10^{-3}M). This effect was time-dependent (**Figure 6A**), reaching a maximal level by 20 min before subsequently declining. The extent of the effect of carbachol was dependent on the level of receptor expression; with lower levels of doxycycline associated with a greater effect of carbachol (**Figure 6B**). This reflected that at higher receptor expression levels the basal htrFRET signal was higher than at lower expression levels (**Figure 6B)** and in this situation carbachol produced a more limited effect on the htrFRET signal (**Figure 6B**). The effect of carbachol on the htrFRET signal corresponding to cell surface VSV-G-SNAP-hM_3WT dimers/oligomers was selective. Clozapine-N-oxide was without effect on the htrFRET signal (**Figure 6A**) and whilst atropine (1 x 10^{-5}M) produced a small reduction in the basal htrFRET signal in some experiments (**Figure 6A**) this was not observed consistently. The effect of carbachol was concentration-dependent with EC_{50} = 3.3 +/- 1.1 x 10^{-4}M (mean +/- SEM, n = 3) (**Figure 6C**). Studies in which carbachol was allowed to compete with [^{3}H]QNB to bind to VSV-G-SNAP-hM_3WT in membranes of cells induced to express this construct showed that this potency corresponded to the lower of two affinity states for carbachol (**Figure 6D**). Acetylcholine, the endogenous agonist of the M_3 muscarinic receptor, was also able to increase the htrFRET signal as extensively as carbachol in cells expressing VSV-G-SNAP-hM_3WT and was some 60 fold more potent than carbachol in so doing (EC_{50} = 5.8 x 10^{-6}M) (**Figure 6E**). Interestingly, in cells induced to express VSV-G-SNAP-hM_3RASSL, clozapine-N-oxide increased the basal htrFRET signal in a concentration-dependent fashion (**Figure 7A**) whereas neither carbachol nor atropine had any effect (**Figure 7B**).

DISCUSSION

It is now well established that many, and perhaps all, rhodopsin-like, family A GPCRs can form dimers and/or higher oligomers (4-7). However, the significance of this remains uncertain because it is not inherently required to allow interaction with a G protein (1-3). Indeed, there is evidence that monomeric family A GPCRs may actually mediate G protein-dependent signals more effectively than dimers (2). Signals from GPCRs may also be generated in G protein-independent fashion (39), but it remains to be established if such signals can also be transduced by monomeric GPCRs.

A further topic that has attracted considerable attention is the question of whether ligands modulate the quaternary organization of GPCRs. Published data on this topic are highly variable (5-8). Given that interactions between individual protomers of class A receptor dimers/oligomers are not generally based on covalent interactions (4-5) then there is clear potential for monomer-multimer equilibria to be altered by the binding of receptor ligands. This reflects that agonist binding must alter receptor conformation (40) to induce states of the receptor able to interact more effectively with G proteins and other GPCR-interacting proteins. Although many studies have suggested that ligand binding to receptors does not produce substantial effects on GPCR quaternary structure (4-7), a

considerable number of observations of ligand modulation of GPCR dimers/oligomers exist in the literature. These include effects of an antagonist/inverse agonist drug to promote the production of a high affinity dimeric state of the M_1 muscarinic receptor from receptor monomers (25) and the concept that the β_2-adrenoceptor exists predominantly in a basal tetrameric state that is unaffected by either agonist or antagonist ligands whilst inverse agonists enhance tighter packing of the protomers and/or the formation of more complex oligomers by reducing conformational fluctuations in individual protomers (41). Other studies are consistent with agonist ligands promoting conformational alterations in pre-existing GPCR dimers/oligomers (40) and both enhancing and reducing dimerization (4-7, 25, 42-44).

It is clearly possible that such variation reflects intrinsic differences in the organization and affinity between protomers of different GPCRs. For example, fluorescence recovery after photobleaching microscopy has been applied to conclude that the β_2-adrenoceptor forms stable complexes whilst the β_1-adrenoceptor displays only transient interactions (45). However, given the range of approaches used to detect interactions between GPCRs and potential regulation by ligands, it is also possible that different techniques might be more or less well suited. Resonance energy-based approaches have dominated the field in recent years (27-29, 46) and studies have generally added energy acceptor and donor moieties to the intracellular C-terminal tail of the GPCR(s) being studied. Strengths and weaknesses of this have been reviewed (28) and debated (47-48). One of the recent additions to the armorium of approaches is a htrFRET method that takes advantage of the capacity of small proteins based on mammalian O^6-alkylguanine-DNA-alkyltransferase to be covalently modified with FRET-competent energy donor and acceptors (31). Via addition of such a SNAP tag to the extracellular N-terminus of class C GPCRs Maurel et al., (32) were able to confirm the presence of cell surface dimers of metabotropic glutamate receptor subtypes. They also used this approach to provide some preliminary data on dimerization of class A receptors (32). Herein, we have extended this to explore the presence and regulation of dimeric/oligomeric complexes at the surface of cells stably expressing forms of the M_3 muscarinic acetylcholine receptor and compared the results with those obtained via more conventional FRET-imaging based studies. A key feature of the FRET imaging studies was to employ the inducible expression of DNA located at the Flp-In™ locus of Flp-In™ T-REx™ 293 cells (33-35). This allowed us to regulate expression of one form of the M_3 muscarinic receptor in the presence of an unaltered amount of a second form in the same cells, rather than attempting to control relative expression levels in a substantial series of transient co-transfection studies. Transient transfection into heterologous cell lines of GPCRs in general and, in particular, of the type of highly modified forms used for resonance energy transfer studies, often results in incomplete folding and their retention in the ER and Golgi. This is a major issue in efforts to explore dimerization in so-called 'saturation' resonance energy transfer studies (28). These require a series of measurements in cells expressing differing ratios of energy-donor and energy-acceptor species. Therefore, the linkage of the energy donor and acceptor species to the C-terminal tail of the GPCRs in question results in signal being recorded from intracellular locations as well as the cell surface. A second key feature of the current studies was the combined use of wild type and RASSL forms of the M_3 muscarinic receptor to take advantage of selective agonist pharmacology. One minor limitation of the M_3 muscarinic receptor RASSL is that it binds conventional antagonist ligands less well than the wild type receptor. This increased the concentration of [^{3}H]QNB needed in the ligand binding studies that were used to define expression levels and receptor pharmacology. However, with good practise the pharmacological characteristics of this variant can be fully defined. This is important because although the affinity of [^{3}H]QNB was 40 fold lower for the RASSL forms of the receptor compared to the wild type, variation in affinity for the widely used muscarinic receptor antagonist atropine was only 3 fold. Variation in ligand affinity at the modified receptor is defined, therefore, by the identity of the specific ligand and must be determined directly for each compound being studied.

Both wild type and RASSL forms of the M_3 muscarinic receptor suitable for FRET imaging were expressed predominantly at the cell surface of Flp-In™ T-REx™ 293 cells when they were induced. Furthermore, strong FRET signals between these froms at the cell surface membrane were obtained in cells engineered to allow their co-expression. However, it should be noted that increasing FRET donor amounts in the presence of a fixed level of FRET acceptor resulted in a bell-shaped curve of ratiometric

FRET signal. This is not surprising. Higher levels of donor would be expected to result in a greater proportion of non FRET-productive donor-donor interactions that are anticipated to eventually limit or out-compete productive donor-acceptor interactions. In these studies carbachol caused a substantial reduction in ratiometric FRET signal. This is consistent with either alteration in the organizational structure of preformed WT-RASSL M_3 receptor complexes or the dissociation of such complexes. By contrast, the antagonist atropine did not modulate such signals substantially. Intra-molecular GPCR FRET sensors, constructed in a single GPCR protomer, are often used to detect agonist-induced alterations in FRET signal corresponding to relative movements of the intracellular ends of transmembrane helices that are believed to promote interaction with a G protein (49-51). Furthermore, relative re-orientation of the transmembrane helices that are believed to be contact interfaces within GPCR dimers/oligomers have been detected upon addition of agonist by a number of means (41, 52-53). However, in many studies employing FRET or BRET, limited overall effects of GPCR ligands have been noted and interpreted to indicate that GPCR dimers/oligomers are present constitutively and not regulated acutely (5, 21, 54). Surprisingly, unlike carbachol, clozapine N-oxide did not alter FRET signal in cells induced to co-express the hM_3 receptor variants. Given that FRET signals in these cells must reflect complexes containing at least one wild type and one RASSL mutant M_3 receptor it might have been anticipated that agonist occupancy of either type of protomer would result in equivalent effects on aspects of complex re-organization. This reflects that there should be reciprocity in regulation between components of a protein complex (55). We do not have a clear explanation for why this was not observed. A number of possibilities exist. For example, although clozapine N-oxide acted as an apparent full agonist at the RASSL variant in the Ca^{2+} mobilization studies, it may, because of issues of receptor reserve, not truly have the same efficacy as carbachol at the wild type receptor. However, it was as effective at causing internalization of the RASSL variant from the surface of the cells as was carbachol in promoting internalization of the wild type receptor. Equally, it may be that the cell surface complex detected by these studies is not a simple 1:1 wild type/RASSL dimer. Indeed, there is growing evidence that at least certain class A GPCRs, including muscarinic receptors, can exist as higher-order complexes containing at least 4 protomers (41, 52-53, 56).

In contrast to the FRET imaging studies, those based on the Tag-lite™ system produced evidence consistent with either significant agonist-induced re-organization within constitutive M_3 receptor quaternary structure or, perhaps more interestingly, agonist-induced enhancement of dimerization/oligomerization. Firstly, these effects were produced only by pharmacologically appropriate agonists, i.e. carbachol and acetylcholine at the wild type receptor and clozapine-N-oxide at the RASSL variant. Moreover, agonist potencies in these studies were consistent with receptor occupancy. However, as with the FRET imaging studies, clozapine-N-oxide was less effective at the RASSL variant than either carbachol or acetylcholine at the wild type receptor complex. Secondly, effects of carbachol were most pronounced at lower levels of receptor expression. This is at least consistent with the concept that the M_3 receptor displays a greater propensity to form oligomeric structure at higher density. In such a situation agonist might not be able to promote this further, whilst at lower receptor density there is less quaternary organization but this is promoted by agonist binding. One further curiosity of these observations was the time-dependence of the effects. These were much slower than the anticipated association constant for the ligand. Interestingly, FRET studies on purified β_2-adrenoceptors have also shown slow time-dependent effects of ligands on intra-molecular movement between transmembrane helices (57) but this is assumed to reflect the artificial environment needed to perform the studies. By contrast, intact cell intra-(50) and inter-(58) molecular FRET studies on the movement of receptor helices are much more consistent with time courses of physiological function.

These results have major implications for our understanding of ligand regulation of GPCR quaternary structure and it will be of great interest to see if similar observations are seen when studying other closely and less closely related GPCRs, both in terms of homo- and hetero-meric pairings. They also indicate that conclusions as to the direction of effect of ligands on such GPCR complexes may depend on the approach used.

FOOTNOTES

These studies were supported by the Biotechnology and Biosciences Research Council (grant BB/E006302/1) and the Medical Research Council (grant G0900050).

Abbreviations: CNO, clozapine-N-oxide; FRET, fluorescence resonance energy transfer; GPCR, G protein-coupled receptor; htr(FRET), homogenous time-resolved (FRET); RASSL, Receptor Activated Solely by Synthetic Ligand.

FIGURE LEGENDS

Figure 1 Generation and pharmacological characterization of Flp-In™ T-REx™ 293 cells able to express forms of the wild type or RASSL M_3 muscarinic acetylcholine receptor on demand
Flag-hM_3WT-Citrine (**1A, 1C**) or myc-hM_3RASSL-Cerulean (**1B, 1D**) were inserted into the Flp-In locus of Flp-In™ T-REx™ 293 cells and pools of positive cells selected. No visible expression of either construct was observed in the absence of the antibiotic doxycycline (**1A, 1B, -dox and bright field images**) but cell surface delivery of both was produced after addition of doxycycline ((**1A, 1B, + dox)**. Elevation of $[Ca^{2+}]_i$ in response to varying concentrations of either carbachol (Cch) or clozapine-N-oxide (CNO) was assessed in both un-induced and doxycycline-treated cells (**1C, 1D**), means +/- SEM, n = 4.

Figure 2 Generation and characterization of Flp-In™ T-REx™ 293 cells able to express inducibly the RASSL M_3 muscarinic acetylcholine receptor in the presence of constitutive expression of wild type M_3 muscarinic acetylcholine receptor
Cells harboring myc-hM_3RASSL-Cerulean at the Flp-In locus as in Figure 1 (**blue**) were subsequently further transfected with Flag-hM_3WT-Citrine (**yellow**) and clones expressing this construct constitutively and stably were isolated. **A.** shows the inducible nature of the RASSL variant (**+ dox versus – dox**). **B.** Membranes from these cells were isolated after treating with doxycycline for varying periods of time, resolved by SDS-PAGE and immunoblotting with anti c-myc (**upper panel**), anti-Flag (**middle panel**) or anti-GFP (that identifies both Cerulean FP and Citrine FP) (**lower panel**). (Arrowheads show the position of the 105 kDa molecular mass marker). **C.** Elevation of $[Ca^{2+}]_i$ in response to varying concentrations of either carbachol (Cch) or clozapine-N-oxide (CNO) was assessed in both RASSL un-induced (**- Dox**) and doxycycline-treated cells (**+ Dox**) means +/- SEM, n = 4. **D.** Images of Citrine FP (**green**), Cerulean FP (**red**) and merging of these images (**merge**) from doxycycline-induced cells were used to construct correlation analyses of color overlap (**right hand picture**).

Figure 3 FRET analysis of interactions between variants of the human M_3 muscarinic acetylcholine receptor
A and **B**. Co-expression of myc-hM_3RASSL-Cerulean (donor) with Flag-hM_3WT-Citrine (acceptor) resulted in raw and corrected (c) FRET signals. Such images were used to calculated ratiometric FRET and how this was modulated by controlling the relative levels of donor to acceptor expression by treatment of cells with varying concentrations of doxycycline. **C**. Levels of acceptor (**yellow**) and donor (**blue**) were quantitated at the cell membrane. **D**. Quantitation of ratiometric FRET signals (Table) and immunological detection of the acceptor (**upper panel**) and donor (**lower panel**) at various doxycycline concentrations are displayed (arrowhead indicates the position of the 105 kDa molecular mass marker). **E.** Radiometric FRET at the cell membrane was measured after treatment with the ligands carbachol, atropine and CNO subsequent to induction of expression of myc-hM_3RASSL-Cerulean with100 $ng.ml^{-1}$ of doxycycline.

Figure 4 Generation and characterization of Flp-In™ T-REx™ 293 cells able to express SNAP-tagged variants of human M_3 muscarinic acetylcholine receptor
A. Flp-In™ T-REx™ 293 cells able to express in an inducible fashion VSV-G-SNAP- hM_3WT (**left hand panels**) or VSV-G-SNAP- hM_3 RASSL (**right hand panels**) are shown. Following receptor induction these were treated with the cell permeant SNAP substrate SNAP-505 (**upper panel and green**), an anti-SNAP antibody labeled with Alexa 594 (**middle panel and red**) or such images were merged (**lower panels**). Cell nuclei are shown in blue. **B**. Cells induced as in **A** (top, VSV-G-SNAP-hM_3WT; bottom VSV-G-SNAP- hM_3-RASSL were labeled with the non-cell permeable reagent Cell-Surface-SNAP-488 and treated with carbachol (1×10^{-3}M) or clozapine-N-oxide (1×10^{-4}M) for 0 or 40 minutes and then imaged. Arrowheads focus attention on receptor populations that became internalized in the presence of ligand.

Figure 5 Establishing Tag-Lite™ htrFRET studies to explore receptor dimerization
Cells induced to express differing amounts of VSV-G-SNAP-hM_3WT by treatment with varying concentrations of doxycycline were incubated with a range of concentrations of the Tb^{2+}-cryptate energy donor SNAP-Lumi4-Tb and cell surface binding of this ligand determined by fluorescence

intensity at 620 nm (**A, top**). Using 4nM SNAP-Lumi4-Tb varying concentrations of the energy acceptor SNAP-Red were added to cells induced with varying concentrations of doxycycline (**A, bottom**) to define optimal ratios of energy donor and acceptor to measure receptor homo-interactions. **B**. The concept of the studies is shown for both VSV-G-SNAP-hM_3WT and VSV-G-SNAP-hM_3RASSL. 'd2' is a cisbio trademark for 'a second generation htrf acceptor characterized by an organic motif of approximately 1,000 Da that is highly FRET compatible with Eu^{3+} and Tb^{+2} cryptates'.

Figure 6 Agonists promote structural re-organization and/or dimerization of the M_3 muscarinic acetylcholine receptor

htrFRET studies were conducted in cells induced to express either VSV-G-SNAP- hM_3WT or VSV-G-SNAP-hM_3RASSL. **A**. At VSV-G-SNAP-hM_3WT carbachol (1×10^{-3}M) but not clozapine-N-oxide (1×10^{-4}M) produced a significant increase in basal htrFRET signal, reaching a maximum after 20 min (**A**). Atropine (1×10^{-5}M) produced a small but significant decrease in the signal in some but not all studies. **B.** The extent of effect of carbachol was dependent on the level of receptor expression, with substantially greater effects when VSV-G-SNAP- hM_3WT expression was lower. **C, D**. The effect of carbachol was concentration-dependent (**C**) and corresponded to the lower affinity state for carbachol as assessed in competition binding studies employing [^{3}H]QNB (**D**). **E**. Acetylcholine (Ach) also increased htrFRET signal in a concentration-dependent manner.

Figure 7 Clozapine-N-Oxide promotes structural re-organization and/or enhanced dimerization of the RASSL M_3 muscarinic acetylcholine receptor

Clozapine-N-oxide produced a concentration-dependent increase of htrFRET signal in cells induced to express VSV-G-SNAP-hM_3RASSL after 40 min of treatment, whilst carbachol and atropine were without effect.

REFERENCES

1. Whorton, M. R., Bokoch, M. P., Rasmussen, S. G., Huang, B., Zare, R. N., Kobilka, B., and Sunahara, R. K. (2007) *Proc Natl Acad Sci U S A* **104**, 7682-7687
2. Kuszak, A. J., Pitchiaya, S., Anand, J. P., Mosberg, H. I., Walter, N. G., and Sunahara, R. K. (2009) *J Biol Chem* **284**, 26732-26741
3. Arcemisbehere, L., Sen, T., Boudier, L., Balestre, M. N., Gaibelet, G., Detouillon, E., Orcel, H., Mendre, C., Rahmeh, R., Granier, S., Vives, C., Fieschi, F., Damian, M., Durroux, T., Baneres, J. L., and Mouillac, B. (2010) *J Biol Chem* **285**, 6337-6347
4. Milligan, G. (2008) *Br J Pharmacol* **153 Suppl 1**, S216-229
5. Milligan, G. (2004) *Mol Pharmacol* **66**, 1-7
6. Szidonya, L., Cserzo, M., and Hunyady, L. (2008) *J Endocrinol* **196**, 435-453
7. Dalrymple, M. B., Pfleger, K. D., and Eidne, K. A. (2008) *Pharmacol Ther* **118**, 359-371
8. Milligan, G. (2010) *Curr Opin Pharmacol* **10**, 23-29
9. Kobayashi, H., Ogawa, K., Yao, R., Lichtarge, O., and Bouvier, M. (2009) *Traffic* **10**, 1019-1033
10. Canals, M., Lopez-Gimenez, J. F., and Milligan, G. (2009) *Biochem J* **417**, 161-172
11. Bonner, T. I. (1989) *Trends Neurosci* **12**, 148-151
12. Wess, J., Eglen, R. M., and Gautam, D. (2007) *Nat Rev Drug Discov* **6**, 721-733
13. Conklin, B. R., Hsiao, E. C., Claeysen, S., Dumuis, A., Srinivasan, S., Forsayeth, J. R., Guettier, J. M., Chang, W. C., Pei, Y., McCarthy, K. D., Nissenson, R. A., Wess, J., Bockaert, J., and Roth, B. L. (2008) *Nat Methods* **5**, 673-678
14. Nichols, C. D., and Roth, B. L. (2009) *Front Mol Neurosci* **2**, 16
15. Claeysen, S., Joubert, L., Sebben, M., Bockaert, J., and Dumuis, A. (2003) *J Biol Chem* **278**, 699-702
16. Bruysters, M., Jongejan, A., Akdemir, A., Bakker, R. A., and Leurs, R. (2005) *J Biol Chem* **280**, 34741-34746
17. Armbruster, B. N., Li, X., Pausch, M. H., Herlitze, S., and Roth, B. L. (2007) *Proc Natl Acad Sci U S A* **104**, 5163-5168
18. Guettier, J. M., Gautam, D., Scarselli, M., Ruiz de Azua, I., Li, J. H., Rosemond, E., Ma, X., Gonzalez, F. J., Armbruster, B. N., Lu, H., Roth, B. L., and Wess, J. (2009) *Proc Natl Acad Sci U S A* **106**, 19197-19202
19. Zeng, F., and Wess, J. (2000) *Neuropsychopharmacology* **23**, S19-31
20. Zeng, F. Y., and Wess, J. (1999) *J Biol Chem* **274**, 19487-19497
21. Goin, J. C., and Nathanson, N. M. (2006) *J Biol Chem* **281**, 5416-5425
22. Novi, F., Scarselli, M., Corsini, G. U., and Maggio, R. (2004) *J Biol Chem* **279**, 7476-7486
23. Park, P. S., and Wells, J. W. (2003) *Biochemistry* **42**, 12960-12971
24. Kang, Y. K., Yoon, T., Lee, K., and Kim, H. J. (2003) *Arch Pharm Res* **26**, 846-854
25. Ilien, B., Glasser, N., Clamme, J. P., Didier, P., Piemont, E., Chinnappan, R., Daval, S. B., Galzi, J. L., and Mely, Y. (2009) *J Biol Chem* **284**, 19533-19543
26. Hern, J. A., Baig, A. H., Mashanov, G. I., Birdsall, B., Corrie, J. E., Lazareno, S., Molloy, J. E., and Birdsall, N. J. (2010) *Proc Natl Acad Sci U S A* **107**, 2693-2698
27. Saenz del Burgo, L., and Milligan, G. (2010) *Expert Opin Drug Discov* **5**, 461-474
28. Milligan, G., and Bouvier, M. (2005) *FEBS J* **272**, 2914-2925
29. Harrison, C., and van der Graaf, P. H. (2006) *J Pharmacol Toxicol Methods* **54**, 26-35
30. Alvarez-Curto, E., Ward, R.J. and Milligan G. (2010) *Ed; Stevens, C.W. Humana Press, New York.(in press)*
31. Gautier, A., Juillerat, A., Heinis, C., Correa, I. R., Jr., Kindermann, M., Beaufils, F., and Johnsson, K. (2008) *Chem Biol* **15**, 128-136
32. Maurel, D., Comps-Agrar, L., Brock, C., Rives, M. L., Bourrier, E., Ayoub, M. A., Bazin, H., Tinel, N., Durroux, T., Prezeau, L., Trinquet, E., and Pin, J. P. (2008) *Nat Methods* **5**, 561-567
33. Stoddart, L. A., Smith, N. J., Jenkins, L., Brown, A. J., and Milligan, G. (2008) *J Biol Chem* **283**, 32913-32924
34. Smith, N. J., Stoddart, L. A., Devine, N. M., Jenkins, L., and Milligan, G. (2009) *J Biol Chem* **284**, 17527-17539

35. Ward, R. J., Alvarez-Curto, E. and Milligan G. (2010) *In 'Receptor Signal Transduction Protocols' 3rd Edition. "Methods in Molecular Biology" series Humana Press. Eds Willars G and Challiss JA (in press).*
36. Youvan, D. C., Silva, C. M., Bylina, E. J., Coleman, W. J., Dilworth, M. R., and Yang, M. M. (1997) *Biotechnology* ***3***, 1-18
37. Lopez-Gimenez, J. F., Canals, M., Pediani, J. D., and Milligan, G. (2007) *Mol Pharmacol* **71**, 1015-1029
38. Shaw, G., Morse, S., Ararat, M., and Graham, F. L. (2002) *FASEB J* **16**, 869-871
39. DeWire, S. M., Ahn, S., Lefkowitz, R. J., and Shenoy, S. K. (2007) *Annu Rev Physiol* **69**, 483-510
40. Vilardaga, J. P., Bunemann, M., Feinstein, T. N., Lambert, N., Nikolaev, V. O., Engelhardt, S., Lohse, M. J., and Hoffmann, C. (2009) *Mol Endocrinol* **23**, 590-599
41. Fung, J. J., Deupi, X., Pardo, L., Yao, X. J., Velez-Ruiz, G. A., Devree, B. T., Sunahara, R. K., and Kobilka, B. K. (2009) *EMBO J* **28**, 3315-3328
42. Cvejic, S., and Devi, L. A. (1997) *J Biol Chem* **272**, 26959-26964
43. Grant, M., Collier, B., and Kumar, U. (2004) *J Biol Chem* **279**, 36179-36183
44. Savi, P., Zachayus, J. L., Delesque-Touchard, N., Labouret, C., Herve, C., Uzabiaga, M. F., Pereillo, J. M., Culouscou, J. M., Bono, F., Ferrara, P., and Herbert, J. M. (2006) *Proc Natl Acad Sci U S A* **103**, 11069-11074
45. Dorsch, S., Klotz, K. N., Engelhardt, S., Lohse, M. J., and Bunemann, M. (2009) *Nat Methods* **6**, 225-230
46. Gandia, J., Lluis, C., Ferre, S., Franco, R., and Ciruela, F. (2008) *Bioessays* **30**, 82-89
47. James, J. R., Oliveira, M. I., Carmo, A. M., Iaboni, A., and Davis, S. J. (2006) *Nat Methods* **3**, 1001-1006
48. Bouvier, M., Heveker, N., Jockers, R., Marullo, S., and Milligan, G. (2007) *Nat Methods* **4**, 3-4; author reply 4
49. Granier, S., Kim, S., Fung, J. J., Bokoch, M. P., and Parnot, C. (2009) *Methods Mol Biol* **552**, 253-268
50. Zurn, A., Zabel, U., Vilardaga, J. P., Schindelin, H., Lohse, M. J., and Hoffmann, C. (2009) *Mol Pharmacol* **75**, 534-541
51. Lohse, M. J., Bunemann, M., Hoffmann, C., Vilardaga, J. P., and Nikolaev, V. O. (2007) *Curr Opin Pharmacol* **7**, 547-553
52. Han, Y., Moreira, I. S., Urizar, E., Weinstein, H., and Javitch, J. A. (2009) *Nat Chem Biol* **5**, 688-695
53. Guo, W., Urizar, E., Kralikova, M., Mobarec, J. C., Shi, L., Filizola, M., and Javitch, J. A. (2008) *EMBO J* **27**, 2293-2304
54. Milligan, G. (2007) *Biochim Biophys Acta* **1768**, 825-835
55. Milligan, G., and Smith, N. J. (2007) *Trends Pharmacol Sci* **28**, 615-620
56. Ma, A. W., Redka, D. S., Pisterzi, L. F., Angers, S., and Wells, J. W. (2007) *Biochemistry* **46**, 7907-7927
57. Granier, S., Kim, S., Shafer, A. M., Ratnala, V. R., Fung, J. J., Zare, R. N., and Kobilka, B. (2007) *J Biol Chem* **282**, 13895-13905
58. Vilardaga, J. P., Nikolaev, V. O., Lorenz, K., Ferrandon, S., Zhuang, Z., and Lohse, M. J. (2008) *Nat Chem Biol* **4**, 126-131

Figure 1

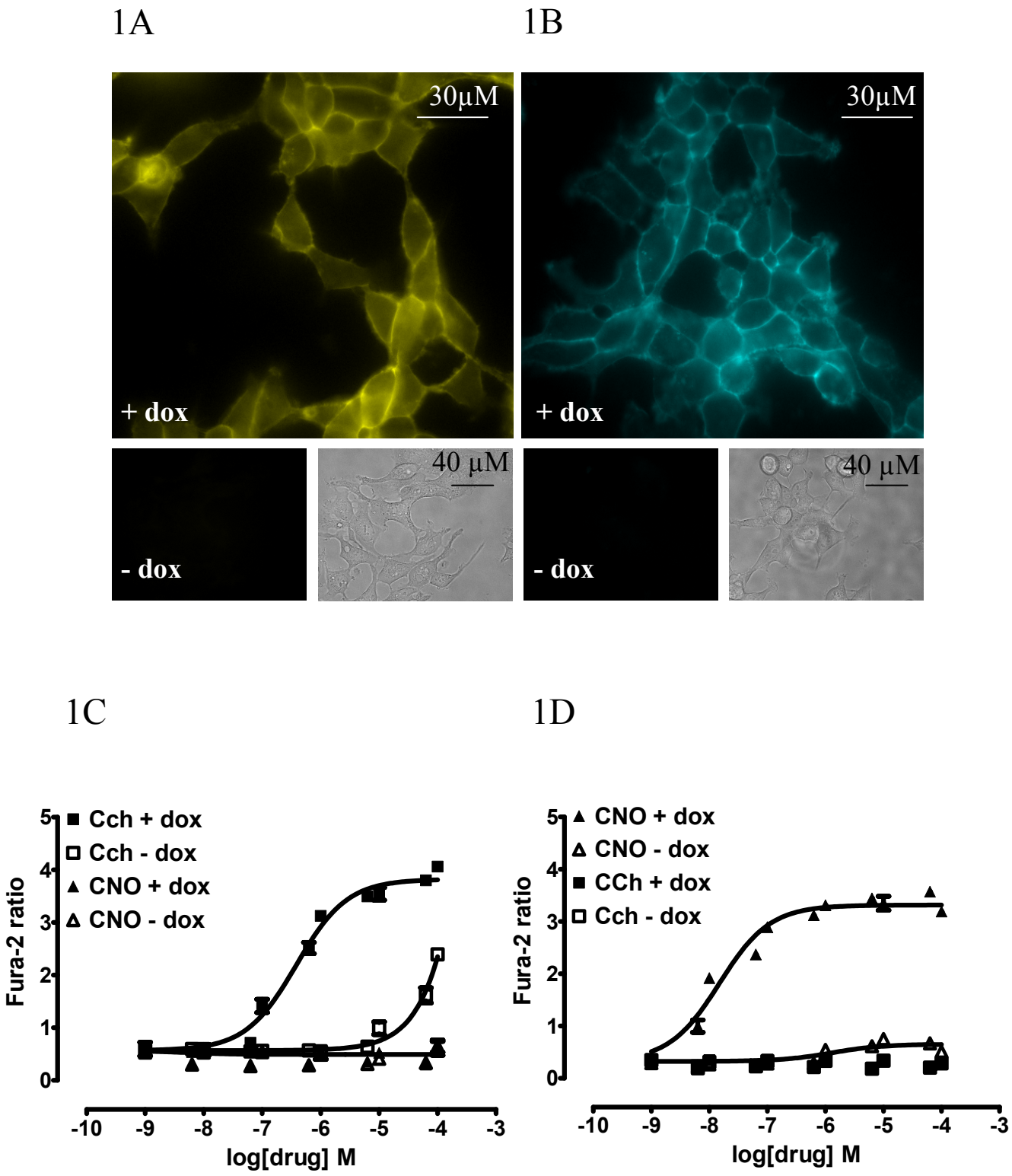
1A
1B
30µM
+ dox
30µM
+ dox
40 µM
- dox
40 µM
- dox
1C
1D
Cch + dox
Cch - dox
CNO + dox
CNO - dox
Fura-2 ratio
log[drug] M
CNO + dox
CNO - dox
CCh + dox
Cch - dox
Fura-2 ratio
log[drug] M

Figure 2

2A

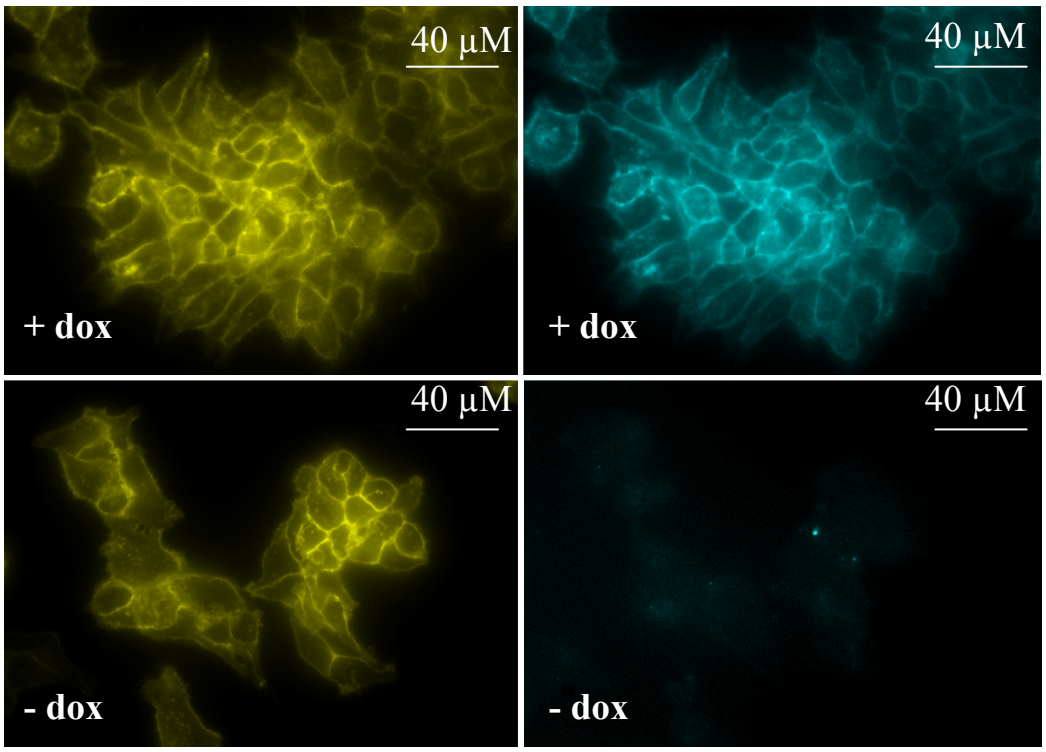

2B

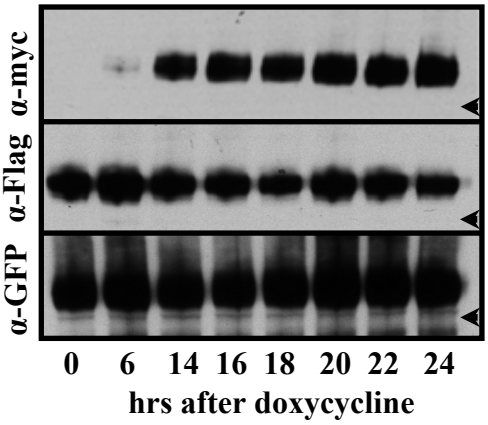

2C

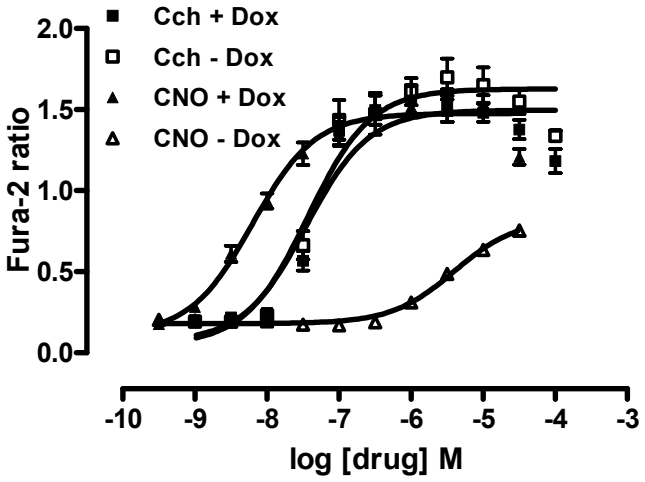

2D

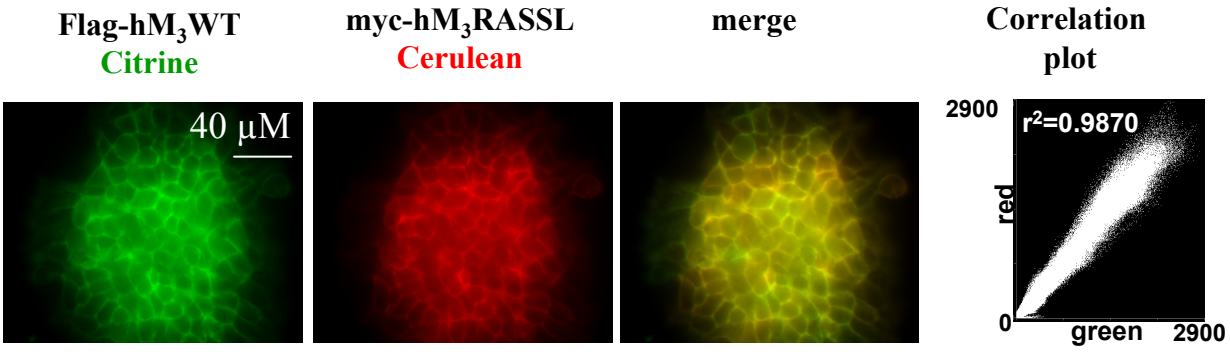

Figure 3

3A

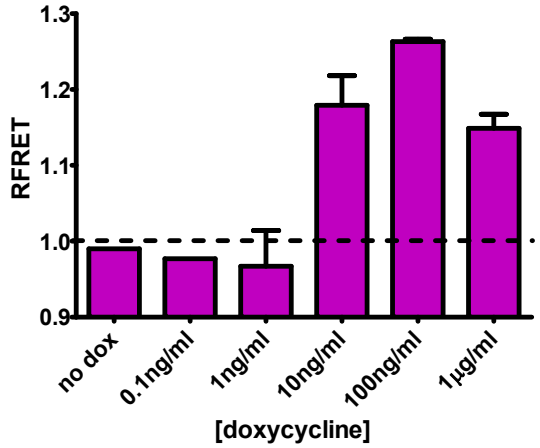

3B

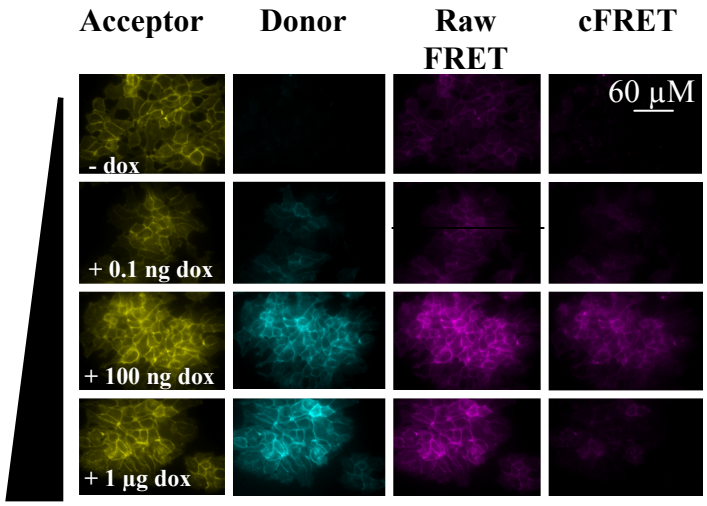

3C

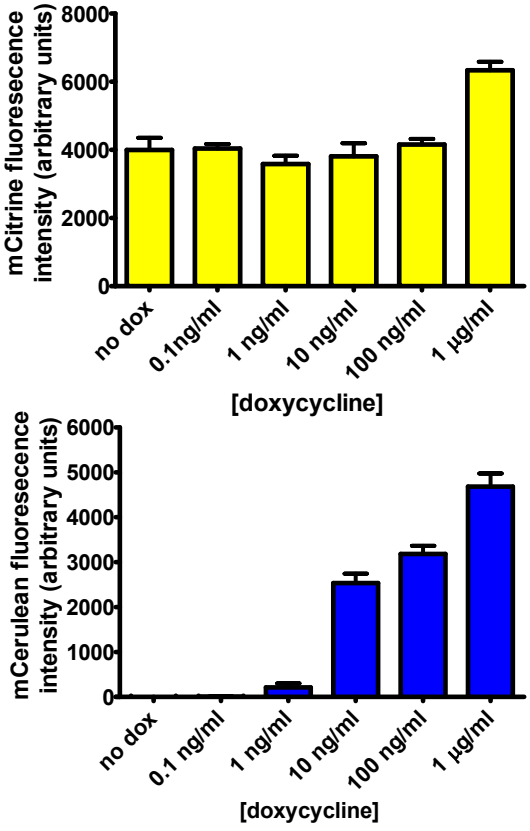

3D

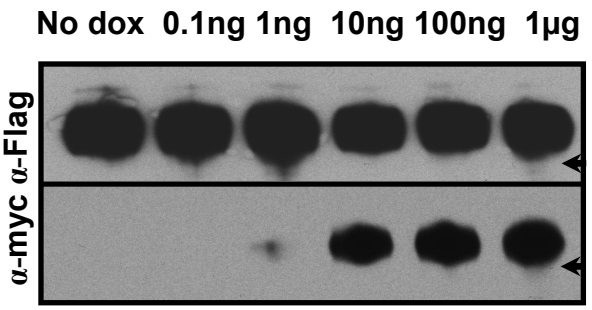

3E

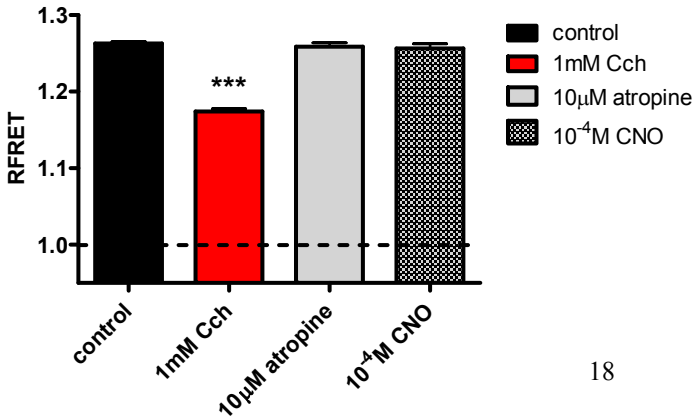

Figure 4

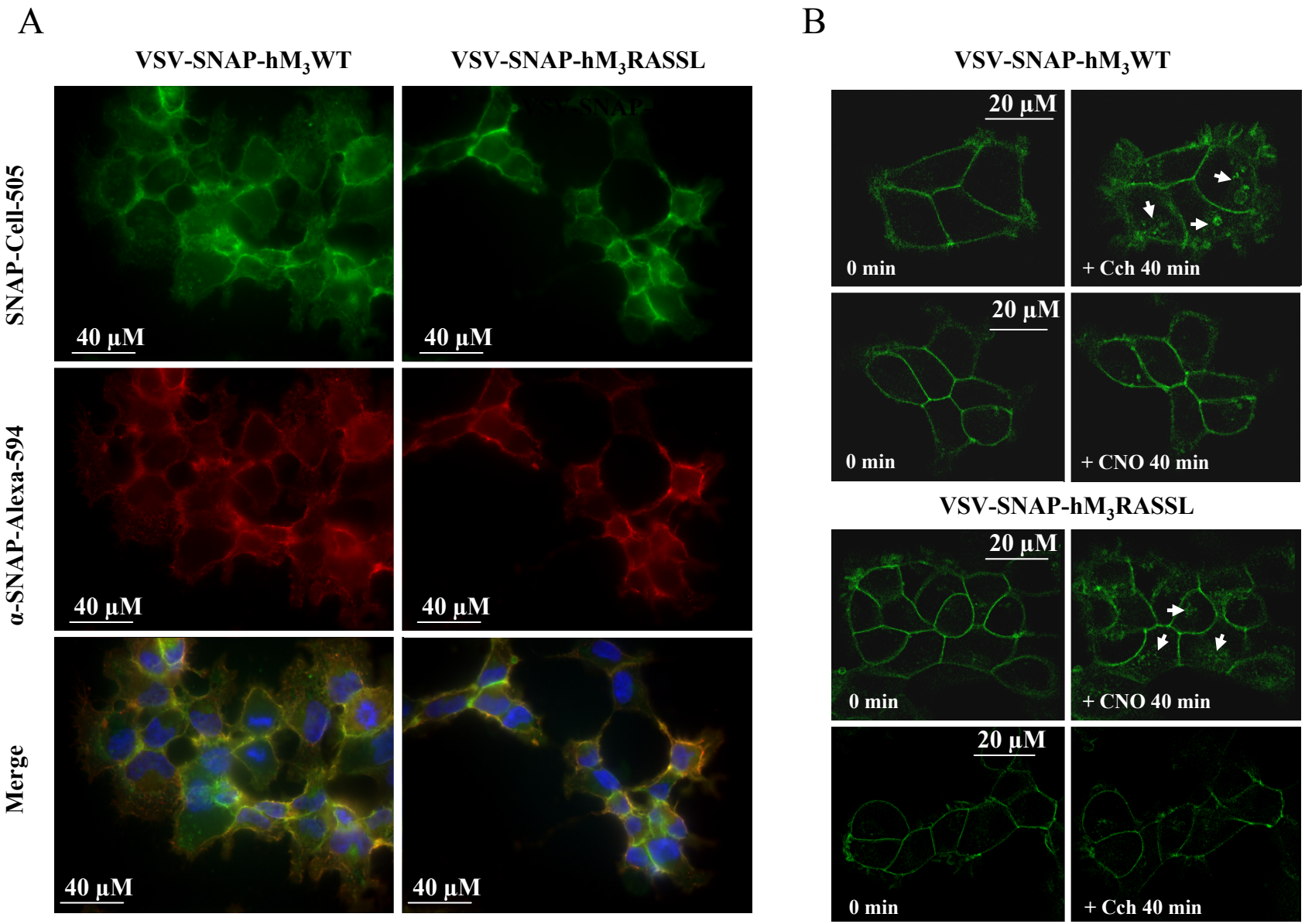
A
VSV-SNAP-hM3WT
VSV-SNAP-hM3RASSL
SNAP-Cell-505
α-SNAP-Alexa-594
Merge
40 µM
B
VSV-SNAP-hM3WT
20 µM
0 min
+ Cch 40 min
+ CNO 40 min
VSV-SNAP-hM3RASSL

Figure 5

5A

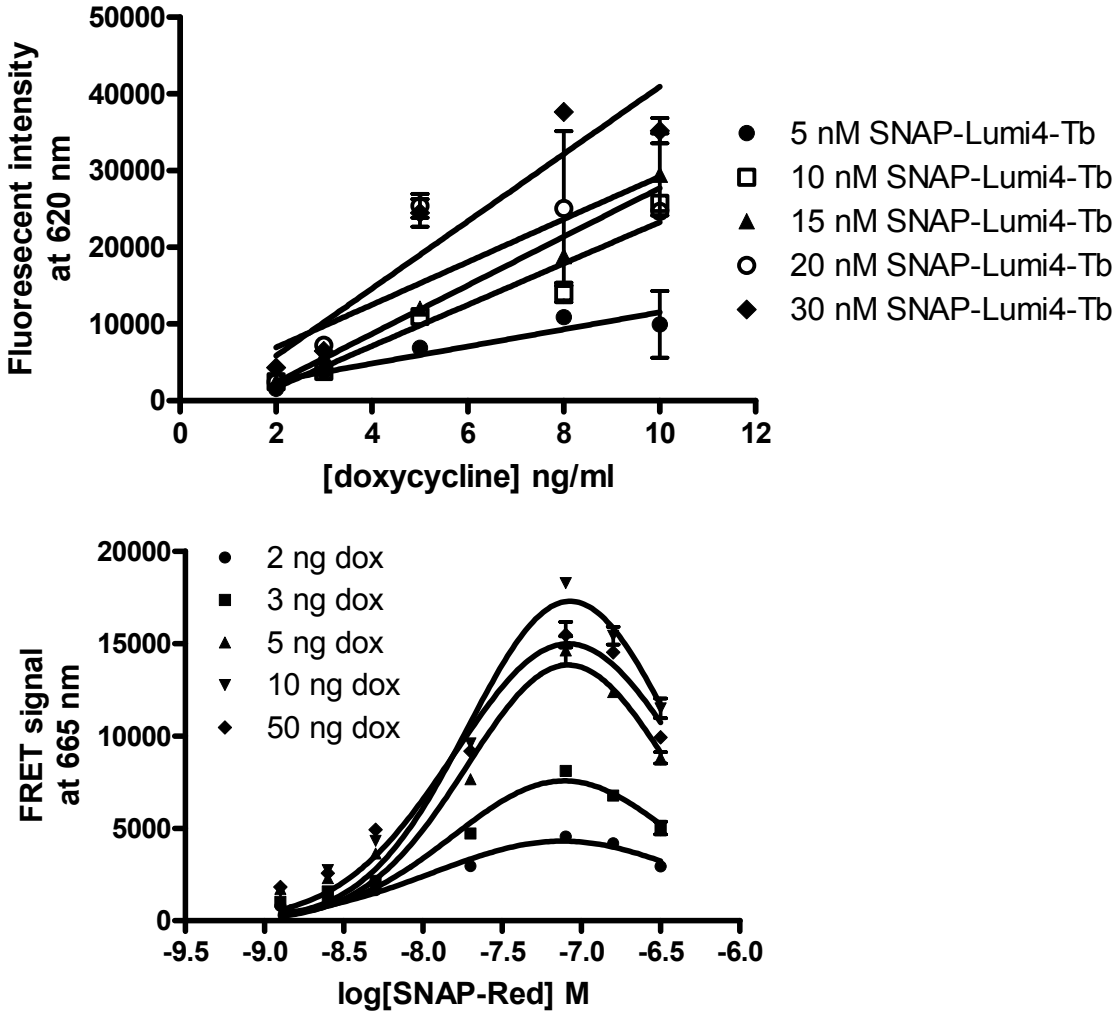

5B

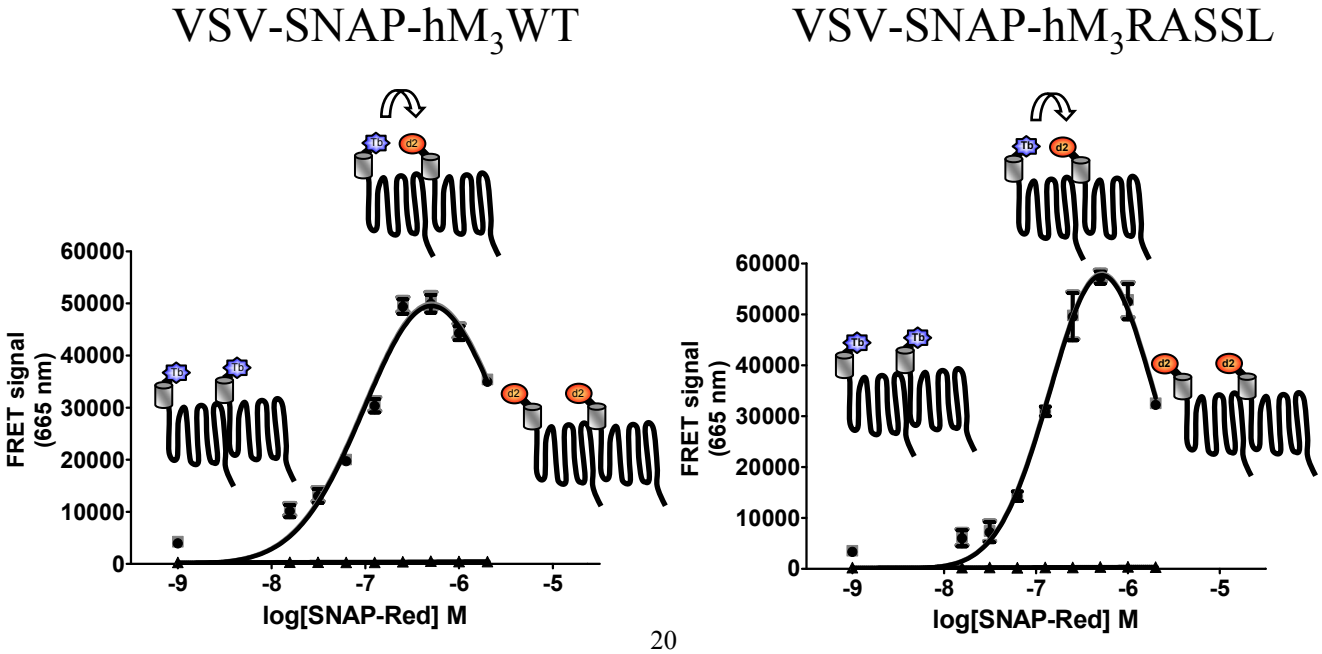

Figure 6

6A

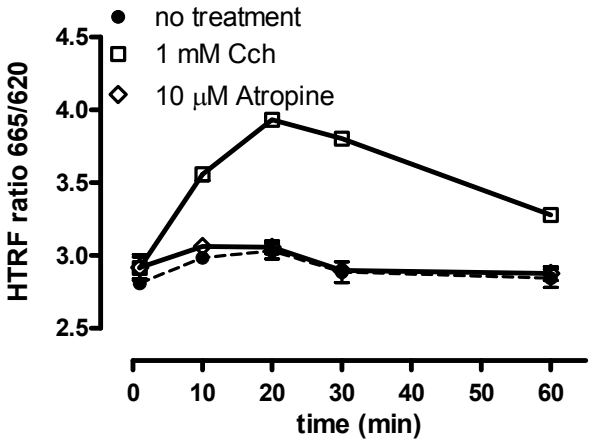

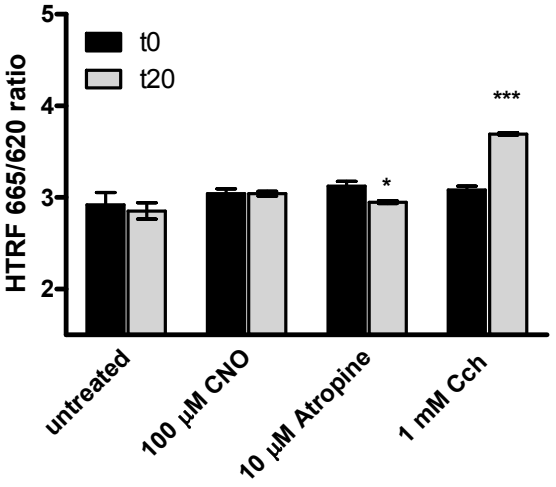

6B

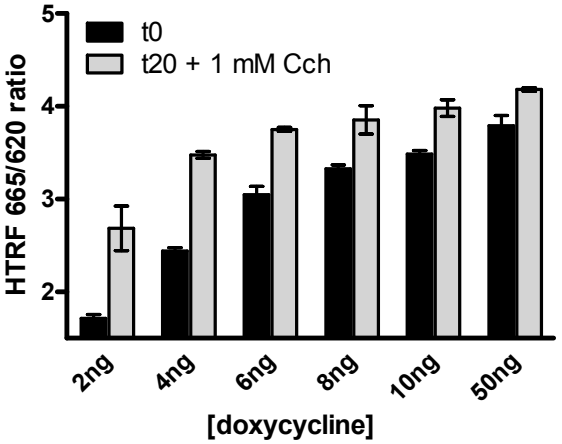

6C

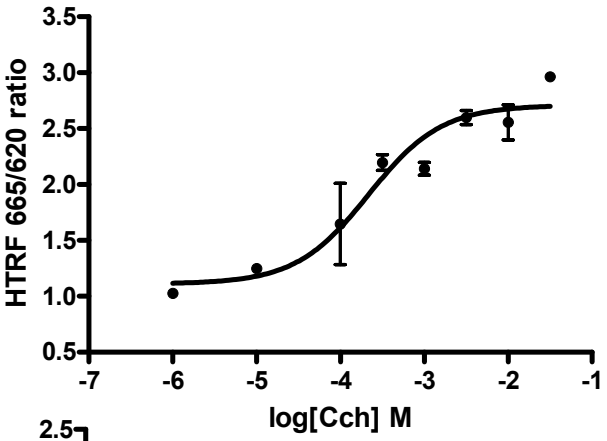

6D

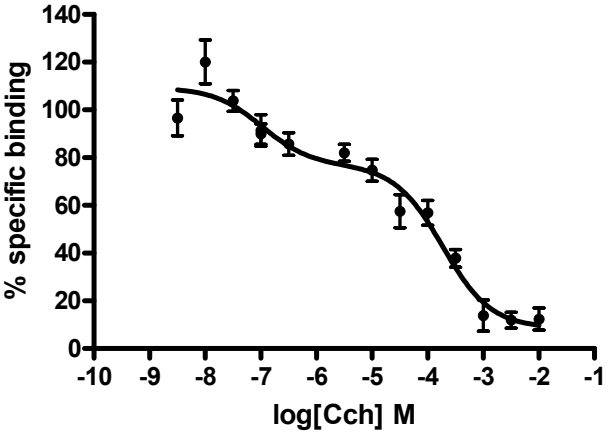

6E

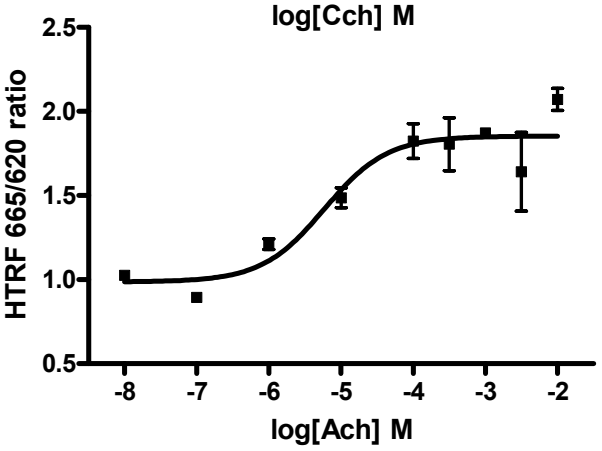

Figure 7

7A

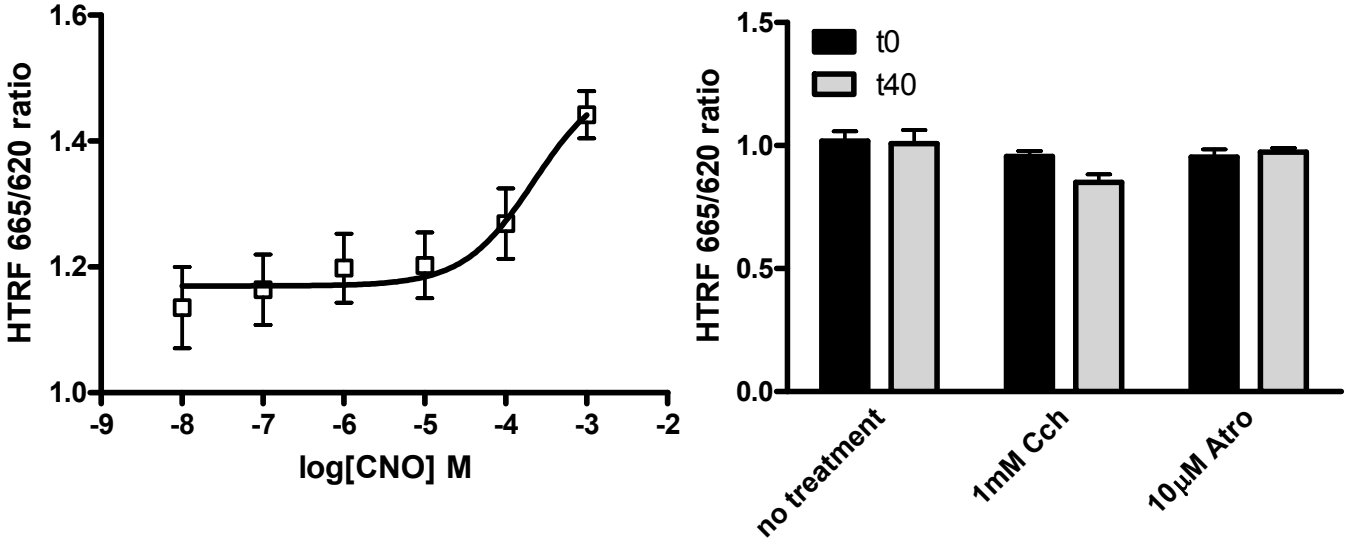
HTRF 665/620 ratio
1.6
1.4
1.2
1.0
-9
-8
-7
-6
-5
-4
-3
-2
log[CNO] M
HTRF 665/620 ratio
1.5
1.0
0.5
0.0
t0
t40
no treatment
1mM Cch
10μM Atro